University of Texas Rio Grande Valley

ScholarWorks @ UTRGV

Mechanical Engineering Faculty Publications and Presentations

College of Engineering and Computer Science

10-13-2014

Fabrication and characterization of silver- and copper-coated Nylon 6 forcespun nanofibers by thermal evaporation

Dorina M. Mihut
Mercer University

Karen Lozano
The University of Texas Rio Grande Valley, karen.lozano@utrgv.edu

Heinrich D. Foltz
The University of Texas Rio Grande Valley, heinrich.foltz@utrgv.edu

Follow this and additional works at: https://scholarworks.utrgv.edu/me_fac

Part of the Mechanical Engineering Commons

Fabrication and characterization of silver- and copper-coated Nylon 6 forcespun nanofibers by thermal evaporation

Dorina M. Mihut[a)] and Karen Lozano
Department of Mechanical Engineering, The University of Texas Pan American, 1201 W University Drive, Edinburg, Texas 78539

Heinrich Foltz
Department of Electrical Engineering, The University of Texas Pan American, 1201 W University Drive, Edinburg, Texas 78539

Silver and copper nanoparticles were deposited as thin films onto substrates consisting of Nylon 6 nanofibers manufactured using forcespinning® equipment. Different rotational speeds were used to obtain continuous nanofibers of various diameters arranged as nonwoven mats. The Nylon 6 nanofibers were collected as successive layers on frames, and a high-vacuum thermal evaporation method was used to deposit the silver and copper thin films on the nanofibers. The structures were investigated using scanning electron microscopy–scanning transmission electron microscopy, atomic force microscopy, x-ray diffraction, and electrical resistance measurements. The results indicate that evaporated silver and copper nanoparticles were successfully deposited on Nylon 6 nanofibers as thin films that adhered well to the polymer substrate while the native morphology of the nanofibers were preserved, and electrically conductive nanostructures were achieved. © 2014 American Vacuum Society. [http://dx.doi.org/10.1116/1.4896752]

I. INTRODUCTION

Scientists have recently intensified their development of polymer nanofibers due to the materials' attractive potential applications and recent methods such as electrospinning and forcespinning® (FS) that have enabled an upscale in their production.[1,2] The potential applications of polymer nanofibers can be further expanded by embedding metallic or ceramic nanoparticles in the polymer nanofibers during their manufacture[3–13] or by surface functionalization of the structures.[14–23] There is recent interest in the mechanical, electrical, and optical properties that can result from using the polymer nanofibers coated with metallic or ceramic nanoparticles. The potential applications of these structures include: catalysis, fuel cells, energy storage, flexible microelectronics, high-performance electrochemical sensors, filtration devices, antistatic, electromagnetic interference shielding clothing, biomedical materials, and wound dressings.[14–29] The forcespinning method[2] uses centrifugal forces to produce nanofibers and has been reported as an attractive method to mass-produce them in the absence of an electric field. The method presents significant advantages, including simplicity, high productivity, cost-effectiveness and versatility in manufacturing nanofibers. The final dimensions and morphology of the nanofibers depend on the spinning velocity, the diameter and configuration of the needle orifice used for production, the selected composition and viscosity of the solution, and the method used for collecting the nanofibers. Different polymeric, metallic, and ceramic oxide nanofibers have been successfully produced by using this method.[3–13] Nylon 6 is a common polymeric material used in many industries, and it was selected for this work due to ease of

manufacture, good mechanical properties, and chemical and thermal stabilities. Silver and copper were the materials used for evaporation and deposition on the Nylon 6 nanofibers considering their attractive electrical properties and thermal conductivities. There are several options for functionalizing polymer nanofibers by metallic nanoparticle deposition on their surface, such as chemical methods, electrodeposition, thermal evaporation and magnetron sputtering. High-vacuum thermal evaporation is an environmentally friendly technique, that ensures high productivity, but it typically requires high temperatures to get the metal to a vapor form. The challenge is to carefully select the working parameters such that the deposition of the metal vapors on the polymer surface is performed at temperatures that preserve the nanofibers. Silver- and copper-coated nanofibers were manufactured and analyzed to evaluate the structures and changes in morphology, electrical conductivities, and the stability over time when placed in an electric field. The electrical conductance/resistance is the fundamental property investigated for the electrical transport phenomena in nanostructured materials. This paper is reporting for the first time the growth of silver and copper thin films on the surface of polymer nanofibers by using high-vacuum thermal evaporation, and specifically, describing the changes in composition, morphology, and electrical properties of metallic-coated structures.

II. EXPERIMENT

Nylon 6 was purchased from Sigma–Aldrich and it was dissolved in formic acid (25% Nylon 6 and 75% formic acid) by stirring until a transparent homogeneous solution was obtained. The polymer solution (2 ml volume) was then injected using a syringe into the spinneret equipped with a

a)Electronic mail: dorinamm@yahoo.com

regular bevel needle and was set to work at a rotational speed of 8000 rpm (rotations per minute) for a total spinning time of 30 s. During the forcespinning process, the Nylon 6 nanofibers were continuously ejected toward the surrounding dish fiber collector to form a nonwoven mat. Polymer square frames with exterior dimensions of $40 \times 40 \times 2$ mm, and 5 mm interior thickness were used to collect the fibers from the dish collector. The frames containing the nanofibers in an isotropic configuration were then placed in the thermal evaporator equipment for metallic depositions. The evaporation sources consisted of high-purity (99.99%) silver and copper pellets placed in tungsten coils located 25 cm away from the polymer substrates. The temperature was continuously monitored during the silver and copper depositions using a thermocouple placed near the nanofibers' surfaces and the deposition parameters were selected to maintain the temperature below 60 °C. A 1.3×10^{-4} Pa (1.0×10^{-6} Torr) pressure was achieved in the thermal evaporator chamber prior to deposition using a cryogenic pump and pressure variation was monitored using an ion gauge. The deposition thickness was monitored *in situ* using a crystal quartz device and silver and copper thin films of 100 or 200 nm thickness were deposited on the nanofiber surfaces. After coating one side, the frames were rotated and coated using the same procedure on the opposite side to ensure uniform coverage of the fibers.

The scanning electron microscopy–scanning transmission electron microscopy (SEM–STEM) Sigma VP (Carl Zeiss AG, Oberkochen, Germany) was used to investigate the morphology of the native, and silver- and copper-coated structures. The phase and crystallinity data for the native and coated structures were obtained at room temperature with a Bruker AXS X-Ray Diffractometer (40 kV, 50 mA) in a θ–2θ scanning mode, using a K_{α} copper radiation source ($\lambda = 1.5406$ Å), with 2θ in the range of $10°$–$90°$. Diffraction patterns were processed through a data evaluation program. An atomic force microscope (AFM) (Digital Instruments Veeco Nanoscope 3D) was used to image the topography of the nanofibers; scanning was carried out in noncontact mode using an antimony-doped silicon cantilever with a nominal spring constant of 0.3 N/m in ambient conditions. Native and silver- and copper-coated mats of Nylon 6 nanofibers with similar dimensions (18×18 mm) were then cut out

from the frames and placed on flat glass insulator substrates. High-conductivity colloidal silver paste (Ted Pella, Inc.) was used in order to create conductive ohmic contact points at two extremities of the metallic-coated mats. Resistance was measured at room temperature using a two-probe resistance meter (BK Precision 5491B 50 000 count multimeter). The DC current–voltage characteristics were obtained using an E5263A 2 channel high-speed source monitor unit (output capability of +/−100 V and +/−200 mA).

III. RESULTS AND DISCUSSION

During the FS process, the centrifugal forces cause a jet of solution to emerge out from the needle and whip around, resulting in the formation of a continuous, thin and long nanofiber. The solvent is evaporated during the rotational process and resulting nanofibers are ultimately dry when they reach the fiber collector surrounding the spinneret assembly. Figure 1(a) shows the FS manufacture process of fabricating Nylon 6 nanofibers using a spinneret with a metallic needle connected to a syringe containing the polymer solution (the prototype system), and (b) shows the pristine Nylon 6 nanofiber nonwoven mat collected on square frames. The average Nylon 6 nanofiber diameter size obtained by using the FS method varies with the spinneret's rotational speed from 100 nanometers to micrometer size; smaller average sizes are generally obtained for higher rotational speeds with the benefit of less beading formation. Figure 2 shows the SEM micrograph of the nonconductive fibrous structure, obtained by using a rotational speed of 8000 rpm. The as-collected nonwoven continuous nanofibers formed a relatively uniform network. The image was obtained with the SEM operating in low-vacuum conditions (24 Pa).

After the FS process, nanofibers were collected as five thin successive layers on square frames using the same direction for collection, and then placed in the thermal evaporator equipment for further deposition of silver or copper thin films. Figure 3 shows the initial stage of nucleation and formation of isolated silver atomic clusters on the native Nylon 6 nanofiber substrate soon after exposing the nanofibers to the silver incident vapor flux. During this initial stage, the silver atoms arriving on the nanofiber surfaces were

FIG. 1. (Color online) (a) Manufacture of Nylon 6 nanofibers using the forcespinning method (prototype system). (b) Pristine Nylon 6 nonwoven mat collected on square frames.
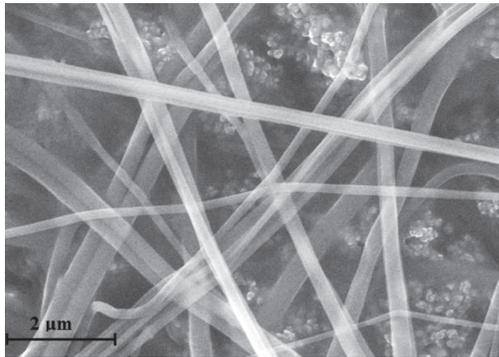
FIG. 2. SEM image of native Nylon 6 forcespun nanofibers (uncoated) obtained at 8000 rpm.

FIG. 4. STEM image of silver nanograins grown on the Nylon 6 nanofiber by thermal evaporation, 100-nm thickness.

condensed and deposited in a similar fashion to the island growth mode,[30] in which silver atoms are more strongly bound to each other than to the substrate. With more evaporation time and additional silver deposition, the islands grew in size and eventually coalesced, forming silver nanograins with multiple facets and orientations, leaving voids between the nanograins. Figure 4 shows an STEM image (8×10^{-4} Pa operating pressure) of silver crystalline nanograins on the polymer nanofibers where the initial voids between isolated structures are starting to fill out. With even more evaporated material, continuous metallic thin films formed on the surface of the Nylon 6 nanofibers. The coating eventually thickened and resulted in polycrystalline thin films composed of multiple nanograins with rougher surface appearances compared to the uncoated nanofibers. With increased coating thicknesses (100 or 200 nm), the nanofibers were completely surrounded by a continuous metallic structure and no delamination of the coating was observed. Figure 5 shows an SEM image of 200-nm thick silver thin films coated on Nylon 6 nanofibers, after the evaporation process was finalized.

A similar coating process was used for copper evaporation on the forcespun nanofibers. The SEM image in Fig. 6 of Nylon 6 nanofibers coated with copper shows smaller

grains and smoother surface appearance when compared to silver thin films of the same thickness. The images of the conductive metallic-coated structures were obtained by operating the SEM in high-vacuum conditions (7×10^{-4} Pa operating pressure). It was observed that for a few of the nanofibers, there were limited regions of reduced or no metallic coatings due to the masking effect from nanofibers located in front of the incoming evaporated flux of atoms. This situation was also observed for the case of silver-coated nanofibers. By comparing the SEM images of uncoated and coated nanofibers, it was observed that the coated surfaces appear to be rougher with well-bonded metallic nanograins of relatively uniform size. The x-ray diffraction (XRD) data were collected for native Nylon 6 nanofibers (uncoated) and for structures composed of metallic thin films evaporated on the nanofibers. The XRD analysis indicated that coated structures are of pure crystalline silver or copper and no oxides formed during the vacuum thermal evaporation process or after exposure to air. Figure 7 shows the nature and phases of native Nylon 6 nanofibers, and 100- and 200-nm thick silver-coated Nylon 6 nanofibers (the base-lines for 100 and 200-nm thick silver coatings were shifted). The graph of native Nylon 6 nanofibers shows the location of pristine Nylon 6 material.[10] The XRD graph for the 100-nm silver coating on Nylon 6 nanofibers at low angles shows the trend of the Nylon 6 substrate material. Silver reflection peaks were present for 2θ values of 38.13°, 44.3°, 64.47°, and 77.52° corresponding to (111), (200), (220), and (311) reflection planes. As the thickness of the silver layer
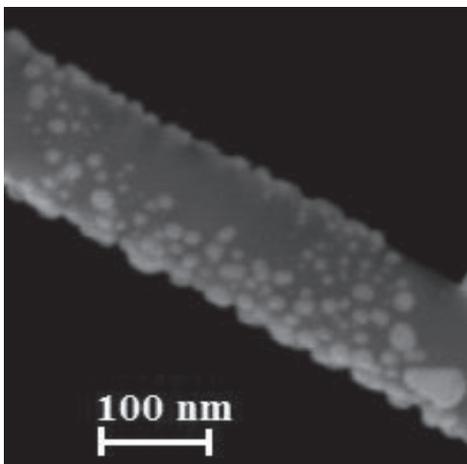

FIG. 3. SEM image of silver atomic clusters deposited on the Nylon 6 nanofiber in the initial stage of the thermal evaporation process.
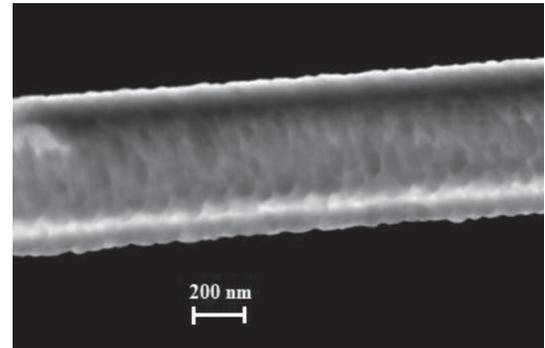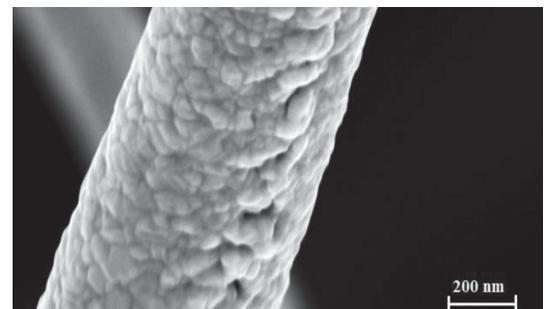

FIG. 5. SEM image of 200-nm silver thin films thermal-evaporated on a single Nylon 6 nanofiber.
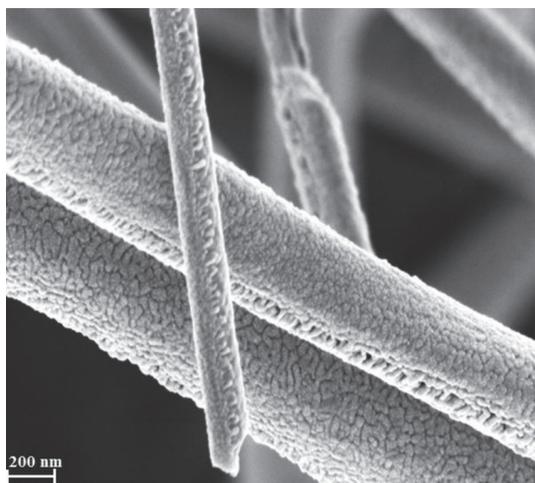
FIG. 6. SEM image of 200-nm copper thin films thermal-evaporated on the Nylon 6 nanofibers' surfaces.

FIG. 8. AFM image of 200-nm thick silver coated on Nylon 6 forcespun nanofiber surfaces.

increased to 200 nm, the relative intensity of the silver peaks also increased. A similar trend was observed for the copper coating (not represented), with copper reflection peaks observed for 2θ values of 43.18°, 50.5°, 74.43°, and 89.93° corresponding to (111), (200), (220), and (311) reflection planes. The values of the XRD detected peaks are close to the indexed values[31,32] both for silver and copper for the respective reflection planes. The AFM image of silver-coated Nylon 6 represented in Fig. 8 shows randomly oriented nanofibers with a web appearance located within the $10.0 \times 10.0 \, \mu m^2$ scanning area. The figure confirms the rough appearance of the surface due to silver grains continuously distributed on the nanofibers surface. The nanofibers are of greater diameter than the uncoated nanofibers.

The electrical properties of native Nylon 6 nanofibers are altered by copper and silver thin film deposition, resulting in surface functionalization of the structures. The sheet resistances of mats consisting of pristine Nylon 6, and silver- or copper-coated Nylon 6 nanofibers were measured after mats were cut out from the frames and placed on insulator glass
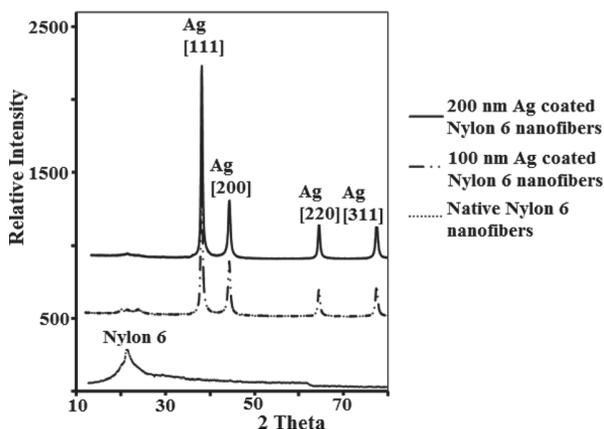

FIG. 7. XRD graphs for native Nylon 6 nanofibers (uncoated), 100 and 200-nm thickness silver coating on Nylon 6 nanofibers' surfaces (the base-lines for 100 and 200-nm thickness silver coatings were shifted).
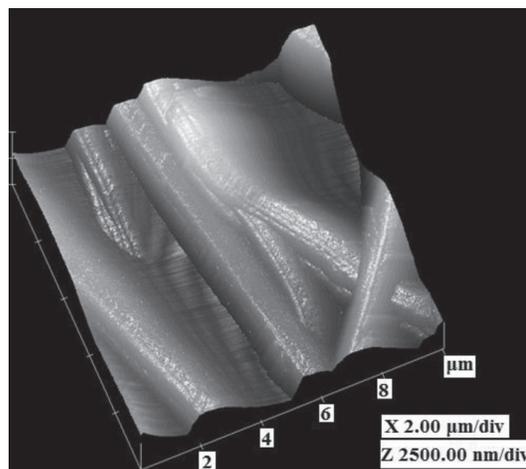
plates. The electrical properties were investigated for mats of similar surface dimensions (18×18 mm) and similar thicknesses. One square mat can be considered to be a simple resistor by analogy with an electric circuit. The ohmic contacts were created using high-conductivity colloidal silver paste applied at two opposite edges of the square surface, allowing measurement of resistance across the square area. Two conductors with known resistance values were used to make the connection from the ohmic contacts to the two-probe resistance meter (BK Precision 5491B 50000-count multimeter). The resistance of the connecting conductors was not included in the final sheet resistance evaluation. It was observed that the sheet resistance of all uncoated force-spun Nylon 6 structures was out of the measurement range with values higher than $10^6 \, \Omega/sq$ showing that pristine Nylon 6 nanofibers are insulators. After depositing 100 nm thickness of silver by thermal evaporation, the sheet resistance of the samples decreased to values of 3–5 Ω/sq indicating the formation of a web of conductive nanowires. It was observed that when the thickness of the silver coating increased to 200 nm, the sheet resistance of all samples decreased further to values between 0.5 and 1.5 Ω/sq due to better metallic coverage of nanofiber surfaces and less voids between the nanograins. A similar trend was observed for copper-coated structures, where the sheet resistance of the samples was from 3 to 8.5 Ω/sq in the case of 100-nm thick copper coatings, and decreased to values of 1–2 Ω/sq for 200-nm copper coating thickness. Higher sheet resistance values were observed for copper-coated than for silver-coated structures due to the generally higher resistance of copper versus silver bulk material. The higher resistance could also be caused by a higher fragility of the copper-deposited nanofibers with more fracture points compared to more continuous and ductile silver-deposited nanofibers. Figure 9(a) presents the SEM image of copper coating (200-nm thickness) on a bundle of Nylon 6 forcespun nanofibers, showing the formation of copper flexible nanoconductors. The resistance of the structures was also monitored while continuously applying a voltage for longer periods of time (up to one week) and
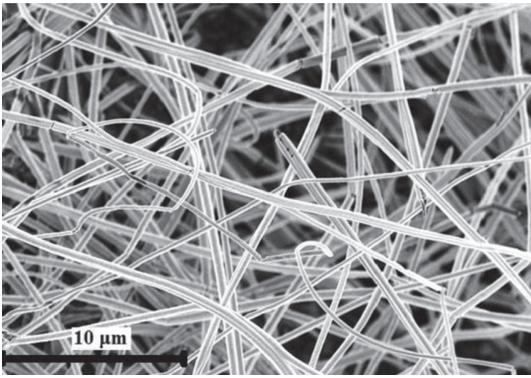
FIG. 9. SEM image of copper-coated bundle of Nylon 6 forcespun nanofibers (200-nm thick coating).

constant resistance measurement was recorded throughout the period indicating good electrical stability of the structures over time. The DC current–voltage characteristics of the metallic-coated nanofibers were analyzed using the same structures as in the case of the two-probe resistance measurement under increased applied voltage in the microvolt (0–10 mV) and volt range (0–2 V). Figure 10 represents typical I–V characteristics of a resistor in the case of 100-nm silver coated Nylon 6 nanofibers in the low (a) and high (b) voltage ranges. All other silver- and copper-coated structures exhibited similar resistor behaviors, showing a proportional current–voltage response. The DC evaluations were performed multiple times at different time intervals and results were consistent over time. The electrical measurement results indicate that Nylon 6 nanofibers were successfully functionalized by silver and copper coating achieved by thermal evaporation with controlled temperatures, without disrupting nanofibers' native morphologies.

IV. SUMMARY AND CONCLUSIONS

In this study, we investigated functionalization of force-spun Nylon 6 nanofibers using silver and copper high vacuum thermal-evaporated thin films deposited under conditions of
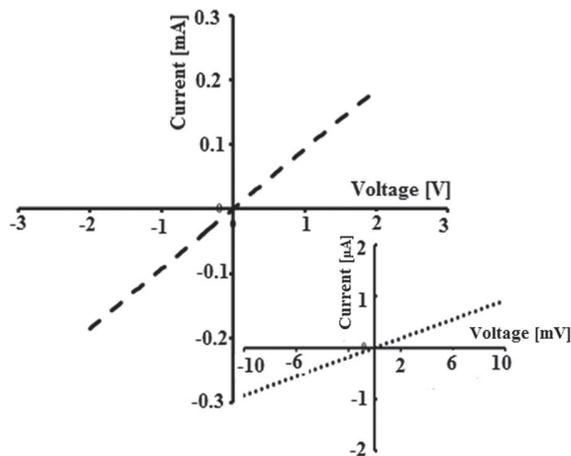

FIG. 10. I–V characteristic for 100-nm thick silver coating on Nylon 6 nanofibers for 0–2 V range and for 0–10 mV range.

controlled temperature and thickness. SEM, STEM, and AFM investigations showed that the thermal evaporation method was successfully used to deposit continuous and uniformly distributed metallic thin films that adhered well to the polymer substrates and morphologies of the native Nylon 6 nanofibers were preserved, with no delamination of the coatings. The surface roughness of the structures increased with increased thickness of the metallic evaporated thin films. The XRD analysis indicated that the coated structures were of pure crystalline silver or copper with no oxide formation during the deposition or after exposure to air. The silver and copper thin films applied on the nanofiber surfaces created a conductive web of nanowires of controllable size; the overall conductivity of the materials was significantly improved with increasing coating thickness and the electrical stability of the structures was maintained over time for all measurements. The surface functionalization achieved here can expand the application potential of polymer nanofibers due to the changes in the electrical properties of the structures. The silver- and copper-coated Nylon 6 nanofiber structures may potentially be applicable for many industrial uses, including sensors, energy storage, flexible microelectronics devices, filtration devices, textile materials with antibacterial properties, antistatic, electromagnetic interference shielding clothing, biomedical materials, wound dressing, and tissue engineering.

[1]Z. M. Huang, Y. Z. Zhang, M. Kotaki, and S. Ramakrishna, Compos. Sci. Technol. **63**, 2223 (2003).
[2]K. Sarkar, C. Gomez, S. Zambrano, M. Ramirez, E. Hoyos, H. Vasquez, and K. Lozano, Mater. Today **13**, 12 (2010).
[3]S. W. Park, H. S. Bae, Z. C. Xing, O. H. Kwon, and M. W. Huh, J. Appl. Polym. Sci. **112**, 2320 (2009).
[4]R. Nirmala, J. W. Jeong, R. Navamathavan, and H. Y. Kim, Nano-Micro Lett. **3**, 56 (2011).
[5]X. Wang, K. Zhang, M. Zhu, H. Yu, Z. Zhou, Y. Chen, and B. S. Hsiao, Polymer **49**, 2755 (2008).
[6]Q. Shi, N. Vitchuli, J. Nowak, J. Noar, J. M. Caldwell, F. Breidt, M. Bourham, M. McCord, and X. Zhang, J. Mater. Chem. **21**, 10330 (2011).
[7]S. D. McCullen, K. L. Stano, D. R. Stevens, W. A. Roberts, N. A. Monteiro-Riviere, L. I. Clarke, and R. E. Gorga, J. Appl. Polym. Sci. **105**, 1668 (2007).
[8]H. Dong, D. Wang, G. Sun, and J. Hinestroza, Chem. Mater. **20**, 6627 (2008).
[9]B. Pant, H. R. Pant, D. R. Pandeya, G. Panthi, K. T. Nam, S. T. Hong, C. S. Kim, and H. Y. Kim, Colloids Surf., A **395**, 94 (2012).
[10]H. R. Pant, D. R. Pandeya, K. T. Nam, W. Baek, S. T. Hong, and H. Y. Kim, J. Hazard. Mater. **189**, 465 (2011).
[11]M. H. Newehy, S. S. A. Deyab, R. Kenawy, and A. A. Megeed, J. Nanomater. **2011**, 626589 (2011).
[12]J. A. Andres, E. Perez, and M. L. Cerrada, Eur. Polym. J. **48**, 1160 (2012).
[13]Y. Xia, P. Yang, Y. Sun, Y. Wu, B. Mayers, B. Gates, Y. Yin, F. Kim, and H. Yan, Adv. Mater. **15**, 353 (2003).
[14]Q. F. Wei, H. Ye, D. Y. Hou, H. B. Wang, and W. D. Gao, J. Appl. Polym. Sci. **99**, 2384 (2006).
[15]Q. Wei, Q. Li, D. Hou, Z. Yang, and W. Gao, Surf. Coat. Technol. **201**, 1821 (2006).

[16]Q. Wei, Q. Xu, Y. Cai, W. Gao, and C. Bo, J. Mater. Process. Technol. **209**, 2028 (2009).

[17]T. Tetsumoto and Y. Gotoh, Sen'I Gakkaishi **66**, 222 (2010).

[18]H. Jiang, S. Manolache, A. C. L. Wong, and F. S. Denes, J. Appl. Polym. Sci. **93**, 1411 (2004).

[19]H. R. Kim, K. Fujimori, B. S. Kim, and I. S. Kim, Compos. Sci. Technol. **72**, 1233 (2012).

[20]Q. F. Wei, F. L. Huang, D. Y. Hou, and Y. Y. Wang, Appl. Surf. Sci. **252**, 7874 (2006).

[21]J. H. Li, X. S. Shao, Q. Zhou, M. Z. Li, and Q. Q. Zhang, Appl. Surf. Sci. **265**, 663 (2013).

[22]R. Nirmala, R. Navamathavan, J. J. Won, K. S. Jeon, A. Yousef, and H. Y. Kim, Mater. Sci. Eng., B **177**, 826 (2012).

[23]S. X. Jiang and R. H. Guo, Surf. Coat. Technol. **205**, 4274 (2011).

[24]S. Yu, U. Welp, L. Z. Hua, A. Rydh, W. K. Kwok, and H. H. Wang, Chem. Mater. **17**, 3445 (2005).

[25]T. Y. Shin, S. H. Yoo, and S. Park, Chem. Mater. **20**, 5682 (2008).

[26]X. Lu, W. Zhang, C. Wang, T. C. Wen, and Y. Wei, Prog. Polym. Sci. **36**, 671 (2011).

[27]Y. J. Song, J. Chen, J. Y. Wu, and T. Zhang, J. Nanomater. **2014**, 193201 (2014).

[28]G. Z. Cao and D. W. Liu, Adv. Colloid Interface Sci. **136**, 45 (2008).

[29]X. Niu, S. P. Stagon, H. Huang, J. K. Baldwin, and A. Misra, Phys. Rev. Lett. **110**, 136102 (2013).

[30]M. Ohring, *Materials Science of Thin Films* (Academic, Boston, 2002).

[31]T. Swanson, Natl. Bur. Stand. Circ. (U.S.) **539**, 23 (1953).

[32]T. Swanson, Natl. Bur. Stand. Circ. (U.S.) **539**, 15 (1953).